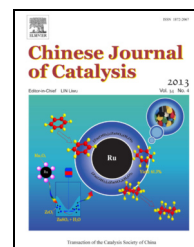


available at www.sciencedirect.comjournal homepage: www.elsevier.com/locate/chnjc

Article

Synthesis of SAPO-35 molecular sieve and its catalytic properties in the methanol-to-olefins reaction

LI Bing^a, TIAN Peng^a, LI Jinzhe^a, CHEN Jingrun^{a,b}, YUAN Yangyang^{a,b}, SU Xiong^{a,b}, FAN Dong^{a,b}, WEI Yingxu^a, QI Yue^a, LIU Zhongmin^{a,*}

^aDalian National Laboratory for Clean Energy, National Engineering Laboratory for Methanol-to-Olefins, Dalian Institute of Chemical Physics, Chinese Academy of Sciences, Dalian 116023, Liaoning, China

^bUniversity of Chinese Academy of Sciences, Beijing 100049, China

ARTICLE INFO

Article history:

Received 30 December 2012

Accepted 30 January 2013

Published 20 April 2013

Keywords:

SAPO-35

Methanol to olefins

SAPO-34

Coke species

Deactivation

ABSTRACT

SAPO-35 molecular sieve samples with different Si contents were hydrothermally synthesized using hexamethylenimine as the template and characterized by XRD, XRF, SEM, MAS NMR, XPS and N₂ physisorption. Three SAPO-35 samples were tested as methanol-to-olefins catalysts. After the reaction, the evolution of coke species was investigated over SAPO-35 and SAPO-34 catalysts with similar Si concentrations. A correlation between the cage size of the molecular sieves and the coke species was obtained.

© 2013, Dalian Institute of Chemical Physics, Chinese Academy of Sciences.
Published by Elsevier B.V. All rights reserved.

1. Introduction

Silicoaluminophosphate molecular sieves (SAPO-*n*) were first synthesized and reported by Union Carbide Corporation (UCC) in 1984 [1]. Due to their mild acidity and special pore structures, SAPO molecular sieves have widespread applications in the chemical industry [2]. SAPO-35, as a member of the family with the levyne-like crystal structure (LEV), is a small pore molecular sieve with a pore diameter of 3.6 nm × 4.8 nm. The framework of SAPO-35 comprises levyne cages connected by single six-membered rings and double six-membered rings. There are two distinct T sites in the framework: one is in the double six-membered ring and the other is in the single six-membered ring. The distribution of these two sites is in the ratio of 2:1 [3]. Due to the special structure of SAPO-35, it has been employed as the catalyst in methanol conversion and

aminomethylation [4–7]. Moreover, SAPO-35 is also explored as an adsorbent for CO₂/CH₄ separation [8,9].

The methanol-to-olefins (MTO) process is the key process to produce light olefins from coal or natural gas. The molecular sieves ZSM-5 and SAPO-34 with eight-membered ring and CHA cages exhibit excellent catalytic performance in the reaction [6,7,10–12]. Other small pore molecular sieves with the eight-membered pore size such as SAPO-17, SAPO-18, and SAPO-35 have also been explored as catalysts for the MTO reaction [7,13,14]. The SAPO-35 molecular sieve showed a faster coking deactivation rate compared with SAPO-34 [4,6]. At present, the correlations between the deactivation process (deposited coke species) and the reaction conditions (such as time and temperature) during the MTO reaction over the SAPO-34 catalyst are relatively clear [15,16]. However, there is no report so far on the deactivation process during methanol conversion

* Corresponding author. Tel/Fax: +86-411-84379335; E-mail: liuzm@dicp.ac.cn

catalyzed by SAPO-35. It is speculated that the activity differences between SAPO-34 and SAPO-35 are due to their different structures. Research on the deactivation during the MTO reaction over SAPO-35 will help understand the effect of the cage structures of the molecular sieves and the deposited coke species.

In this work, SAPO-35 molecular sieves with different Si contents were hydrothermally synthesized by using hexamethyleneimine as the template. The effect of Si content on the physical and chemical properties of the molecular sieves was studied in detail. In addition, three SAPO-35 molecular sieves with different Si contents were chosen as MTO catalysts to investigate the effects of the acidity on the reaction. The evolution of the coke species in the reaction was investigated over both SAPO-35 and SAPO-34 catalysts with similar Si concentrations. The correlation between the cage size of the molecular sieves and deactivation due to the coke species is discussed.

2. Experimental

2.1. Synthesis of molecular sieves

The SAPO-35 molecular sieves were synthesized as reported elsewhere [17]. Pseudoboehmite powder ($w(\text{Al}_2\text{O}_3) = 70$ wt%), sol ($w(\text{SiO}_2) = 31.1$ wt%) and phosphoric acid ($w(\text{H}_3\text{PO}_4) = 85$ wt%) were the aluminum source, silicon source, and phosphorus source, respectively. Hexamethyleneimine (HMI, chemical pure) was used as the template agent. The molar ratio of reactants was $0.96\text{P}_2\text{O}_5:1.0\text{Al}_2\text{O}_3:n\text{SiO}_2:1.51\text{HMT}:55.47\text{H}_2\text{O}$ ($n = 0.1, 0.2, 0.3, 0.5, 0.8, 1.0$). The detailed procedure was as follows. Into a beaker, deionized water, aluminum source, silicon source, phosphorus source, and HMI were sequentially added with vigorous stirring to make the initial gel homogeneous. This was then transferred into a 100 ml stainless steel reactor, which was then sealed and heated at 200 °C for 24 h. After crystallization, the product was collected by centrifugal separation, rinsed with water until the pH level was neutral, and then dried at 120 °C. The samples with different Si contents were denoted as 0.1Si, 0.2Si, 0.3Si, 0.5Si, 0.8Si, and 1.0Si.

2.2. Characterization

X-ray powder diffraction (XRD) measurements were performed using a PANalytical X'Pert PRO X-ray diffractometer with Cu anode, K_α radiation ($\lambda = 0.15418$ nm), voltage of 40 kV and current of 40 mA. The elemental analysis was carried out using a Philips Magix 2424X X-ray Fluorescence Spectrometer (XRF). Morphology images were acquired on a Hitachi S-3400N scanning electron microscopy (SEM). X-ray photoelectron spectroscopy (XPS) was determined employing a Thermo ESCALAB 250Xi X-ray photoelectron spectrometer with Al K_α radiation. The peak of Al 2p at 74.7 eV from Al_2O_3 on the surface of the samples was used as the internal standard. N_2 adsorption measurement was performed on a Micromeritics ASAP 2010 volumetric adsorption analyzer.

^1H MAS NMR experiments were performed on a Bruker Avance III-600 solid phase NMR spectrometer with a proton

resonance frequency of 600.13 MHz by using a 4 mm probe head. One pulse program was used and the $\pi/2$ pulse length was 4.4 μs . The recycle delay time is 10 s. The spin rate was 12 kHz with 32 times sampling frequency. Before the ^1H MAS NMR experiments, all samples underwent vacuum dehydration at 400 °C and $< 10^{-3}$ Pa for 20 h to remove water and impurities in the molecular sieve. The samples were transferred in a nitrogen-filled glove box to the NMR rotator for testing. The quantitative processing of the ^1H MAS NMR data was as follows. A calibration curve for the correlation between peak areas and mass of sample were first made by using adamantane as the external standard. Then the ^1H MAS NMR spectra of the sample with known mass were acquired under identical acquisition conditions. The peak areas of Brönsted acid sites was calculated by Gauss-Lowrance linear fitting to get the density of Brönsted acid sites of the samples from the calibration curve.

2.3. Reaction evaluation

The catalytic properties of the molecular sieves were evaluated using an atmospheric fixed bed equipment. 1.2 g calcined sample (40–60 mesh) was packed in the reactor, which was then purged with nitrogen at 520 °C for 30 min. After purging, methanol solution (40 wt%) was injected into the reactor by a pump. The products were analyzed online using an Agilent 7890A gas chromatograph (GC) with PoraPLOT Q-HT capillary column and FID detector.

2.4. Collections of coke deposits and analysis of coke species

The deposited coke species were collected by stopping the feed after a pre-determined reaction time, unloading the catalysts quickly and then quenching in liquid nitrogen.

The Guisnet method was used for the qualitative analysis of the coke species [18,19]. In a Teflon bottle, 50 mg of catalyst was added to 1 ml HF water solution (20 wt%). After the mixture was shaken well and allowed to sit for 1 h, 0.5 ml dichloromethane was added into the solution. 5 min later, NaOH was added and mixed well. The mixture was then transferred to a separatory funnel and shaken vigorously. The lower layer liquid was collected into a sample vial for GC testing by an Agilent 7890-5975C MSD gas chromatograph-mass spectrometer with a HP-5 capillary column. Each compound was identified using the NIST 08 library.

3. Results and discussion

3.1. Synthesis and characterization of SAPO-35 with different Si contents

The XRD results of the samples are shown in Fig. 1. All the SAPO-35 molecular sieves with different Si contents had the LEV framework structure, as shown by comparing to the standard pattern [7,20]. The relative crystallinity, relative yield, and chemical composition of the SAPO-35 samples with different Si contents are listed in Table 1. The solid yield of the samples increased with increasing amount of SiO_2 in the initial gels.

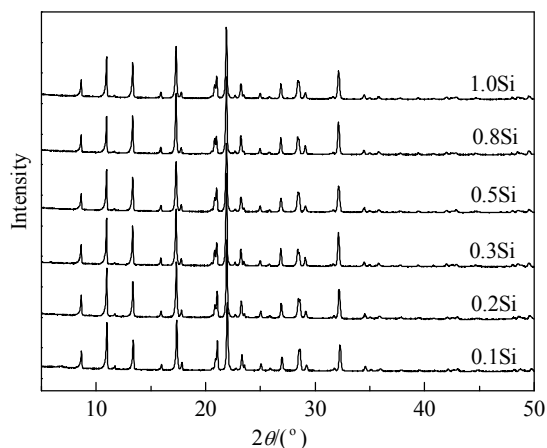


Fig. 1. XRD patterns of the SAPO-35 samples with different Si contents.

However, the crystallinity exhibited first an increase then a decrease trend. 0.3Si sample showed the highest crystallinity. In our previous research on the synthesis of SAPO-34, we also found that samples with 0.2–0.3 Si contents had the highest crystallinity [21]. This suggested that the Si content in the initial gel not only affected the chemical composition of the samples but also the crystallinity. In addition, the XRF elemental analysis results indicated that the Si content of SAPO-35 increased with the increase of Si content in the initial gel. To better correlate the Si contents of the starting materials and products, we introduce a concept of “silicon incorporation” defined as $[\text{Si}/(\text{Si}+\text{Al}+\text{P})]_{\text{product}}/[\text{Si}/(\text{Si}+\text{Al}+\text{P})]_{\text{gel}}$ (shown in Table 1). A descending tendency was found for silicon incorporation in SAPO-35 with the increase of Si content in the starting materials. The 0.1Si sample exhibited the highest silicon incorporation of 1.82. The silicon incorporation decreased to less than 1.0 when the Si content of the initial gel was more than 0.3. Silicon incorporation was only 0.7 when the Si content of the initial gel was 1.0. Therefore, we believed that it is the high silicon incorporation associated with the samples with low Si contents that resulted in their relatively low solid yields. Catlow et al. [22] employed lattice simulation to calculate the energy changes of

Table 1

Relative crystallinity and chemical composition of the SAPO-35 samples with different Si contents.

Sample	Relative crystallinity (%)	Relative yield (%)	Molar composition	Si incorporation*
0.1Si	84	62	$\text{Si}_{0.060}\text{Al}_{0.490}\text{P}_{0.450}$	1.82
0.2Si	94	74	$\text{Si}_{0.079}\text{Al}_{0.497}\text{P}_{0.424}$	1.25
0.3Si	100	86	$\text{Si}_{0.092}\text{Al}_{0.485}\text{P}_{0.423}$	1.01
0.5Si	94		$\text{Si}_{0.122}\text{Al}_{0.487}\text{P}_{0.391}$	0.89
0.8Si	91	95	$\text{Si}_{0.169}\text{Al}_{0.465}\text{P}_{0.367}$	0.80
1.0Si	85	100	$\text{Si}_{0.175}\text{Al}_{0.457}\text{P}_{0.368}$	0.70

*Defined as the molar ratio of $[\text{Si}/(\text{Si}+\text{Al}+\text{P})]_{\text{product}}/[\text{Si}/(\text{Si}+\text{Al}+\text{P})]_{\text{gel}}$.

silicon incorporation in the framework of SAPO-5 molecular sieves and found that highly dispersed and singly substituted silicon was the most stable, followed 5Si and 8Si islands. These results suggested that the energy of Si incorporation in the framework increased with increasing content of substituted silicon, leading to the decreasing ability for silicon incorporation in the framework. Their conclusion is consistent with our experimental results.

The SEM images of the samples with different Si contents are shown in Fig. 2. The SAPO-35 grains presented the typical rhombohedral morphology, but the change of silicon content had a significant effect on the surface roughness of the molecular sieve crystals. With a low silicon content, the molecular sieve surface was relatively smooth. The crystal surface became rough and irregular small holes appeared when the silicon content was increased to 0.8. When the silicon content was 1.0, the surface of the crystal was wrapped by small particles and it showed a ‘core-shell’ structure, which presumably resulted from a secondary crystal growth on the rough surface of the crystal or the enrichment of excessive amorphous silica in the gel on the crystal surface. The surface compositions of the 0.5Si and 1.0Si samples were analyzed by XPS (Table 2). It was found that the crystal surface of these two samples comprised silica, phosphorus oxide, and alumina. The relative silicon content of the surface was higher than that of the bulk phase, and the enrichment of silicon on the high silicon content sample surface was higher. It was thus speculated that the shell of the 1.0Si

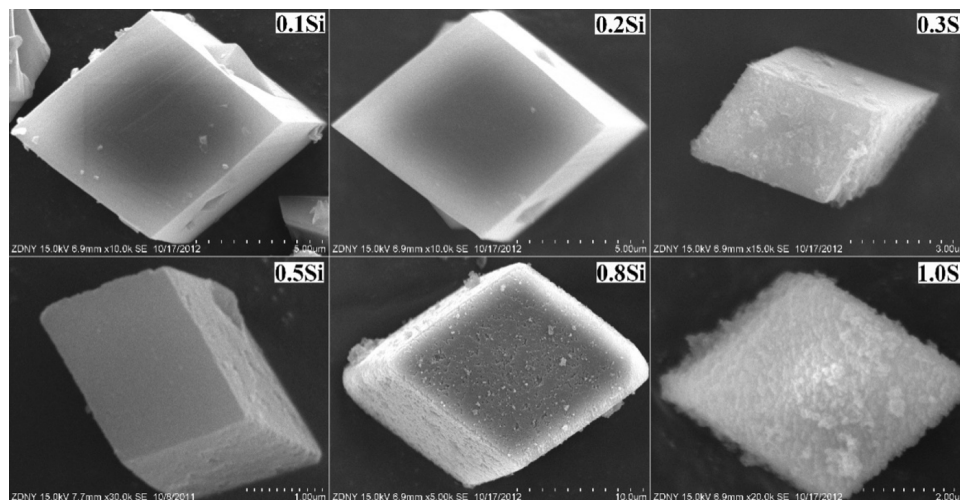


Fig. 2. SEM images of the SAPO-35 samples with different Si contents.

Table 2

Bulk and surface compositions of the SAPO-35 samples with different Si contents.

Sample	Composition		Si _{surface} /Si _{bulk}
	Bulk	Surface	
0.5Si	Si _{0.122} Al _{0.487} P _{0.391}	Si _{0.178} Al _{0.478} P _{0.335}	1.46
1.0Si	Si _{0.175} Al _{0.457} P _{0.368}	Si _{0.275} Al _{0.405} P _{0.320}	1.58

sample grains was formed by a secondary crystal growth on the rough surface of the crystal. Meanwhile, from the silicon enrichment on the SAPO-35 crystal surface revealed by XPS, we can suppose that the distribution of silicon in the SAPO-35 crystals was non-uniform and there was a gradual increase of the silicon content from the inside outwards. We also found a similar situation in the crystallization of SAPO-34 with diethylamine as a template agent [23]. The main reason would be the gradual increase of the gel pH during the synthesis of SAPO molecular sieves. The increase of pH promoted depolymerization of the silicon source in the gel system, thus the ability for silicon incorporation into the molecular sieve framework was enhanced (the pH value of the gel in our synthesis system before and after the crystallization of 0.5Si sample were 5.56 and 8.20, respectively).

Figure 3 and Table 3 show the N₂ adsorption-desorption isotherms, specific surface areas, and pore volumes of the samples with different Si contents. All three samples displayed a high micropore surface area and micropore volume. Moreover, the outer specific surface area and mesopore volume of the samples increased with the increase of silicon contents, which would be due to the rough grain surface of the samples with high silicon contents, as revealed by the SEM images.

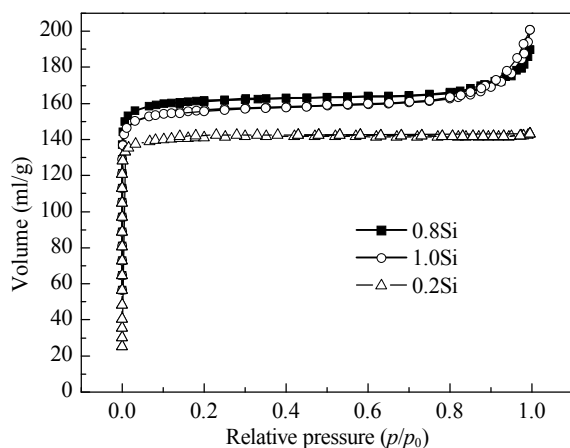

Fig. 3. N₂ adsorption-desorption isotherms of the SAPO-35 samples with different Si contents.

Table 3

Pore structure parameters of the SAPO-35 samples with different Si contents.

Sample	Surface area (m ² /g)			Pore volume (cm ³ /g)		
	Micropore	External	Total	Micropore	Mesopore	Total
0.2Si	443.5	26.3	469.7	0.22	0.01	0.21
0.8Si	497.4	41.0	538.4	0.23	0.05	0.28
1.0Si	475.4	45.8	521.2	0.22	0.07	0.29

3.2. Methanol conversion by SAPO-35 molecular sieve with different Si contents

0.1Si, 0.3Si, and 0.5Si samples were selected for the study of methanol conversion. The results are shown in Fig. 4 and Table 4. The results of the MTO reaction on SAPO-34 (elemental composition is Si_{0.086}Al_{0.493}P_{0.421}) are also listed in Table 4 for comparison. During an initial period, the conversion of methanol on SAPO-35 with different Si contents was maintained at above 99%. The conversion decreased as the reaction time increased and the higher the Si content, the faster the conversion of methanol dropped. The selectivity for ethylene of these molecular sieves gradually rose as the reaction time increased, while the selectivity for propylene decreased. Compared with SAPO-34, SAPO-35 exhibited the characteristic of fast deactivation.

The MTO reaction is a typical acid catalyzed reaction, and the acidity of the molecular sieve plays an important role on the lifetime and the selectivity to light olefins. We determined the amount of Brönsted acid of the three SAPO-35 samples using ¹H MAS NMR (shown in Table 5). Generally, the density of Brönsted acid sites increased in the samples with the increase of the Si contents. Both are almost in a linear relationship. The higher acid density in the samples with higher Si content caused serious side reactions, such as coke deposition and the hydrogen transfer reaction, which shortened the life time of the catalyst and generated more methane and propane. Moreover, the deposited coke species gradually formed during the reaction will decrease the cage size of the molecular sieves, reduce the generation and diffusion rates of molecules with larger diameters, and consequently increase the selectivity for ethylene and decrease the selectivity for propylene.

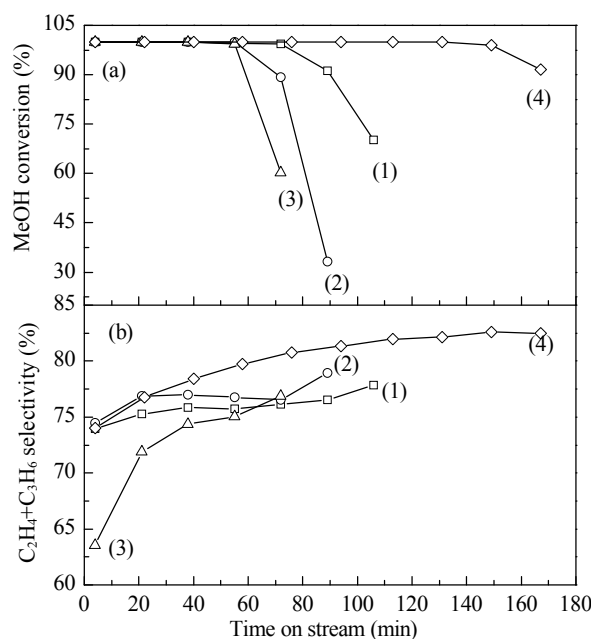

Fig. 4. CH₃OH conversion (a) and C₂H₄+C₃H₆ selectivity (b) in the MTO reaction over SAPO-35 and SAPO-34. (1) 0.1Si; (2) 0.3Si; (3) 0.5Si; (4) SAPO-34. Reaction condition: 450 °C, 40% CH₃OH solution (SAPO-35, WHSV = 2 h⁻¹; SAPO-34, WHSV = 4 h⁻¹).

Table 4

MTO results over SAPO-35 and SAPO-34 molecular sieves.

Sample	TOS (min)	Selectivity (wt%)							
		CH ₄	C ₂ H ₄	C ₂ H ₆	C ₃ H ₆	C ₃ H ₈	C ₄	C ₅₊	C ₂ ⁺ +C ₃ ⁺
0.1Si	4	2.37	37.80	0.27	36.17	1.05	10.42	11.87	73.96
	72 ^a	2.66	43.85	1.02	32.30	1.41	9.24	9.43	76.16
0.3Si	4	2.71	33.94	0.30	40.55	1.31	12.46	8.69	74.50
	55 ^a	3.35	41.38	1.11	35.38	1.48	9.13	8.10	76.75
0.5Si	4	3.43	29.04	0.89	34.48	2.94	13.13	16.07	63.53
	55 ^a	3.43	42.09	1.48	32.95	1.88	8.90	9.16	75.05
SAPO-34 ^b	4	0.96	33.61	0.65	40.38	4.63	15.64	4.08	74.00
	131 ^a	1.49	43.32	0.62	38.80	1.54	11.03	3.10	82.12

 Reaction condition: WHSV = 2 h⁻¹, 450 °C, 40% CH₃OH solution.

^a The catalyst lifetime, which is defined as the reaction duration with >99% CH₃OH conversion.

^b Reaction condition: WHSV = 4 h⁻¹, 450 °C, 40% CH₃OH solution (elemental composition of SAPO-34: Si_{0.086}Al_{0.493}P_{0.421}).

3.3. Analysis of the deposited coke species formed in the MTO reaction over SAPO-35 and SAPO-34

The fast deactivation of SAPO-35 molecular sieve in the methanol conversion reaction indicated that the deposited coke species and their evolution with reaction time on SAPO-35 is different from those on SAPO-34. We selected 0.3Si SAPO-35 to study the deposited coke species following the reaction time and compared these with those generated on SAPO-34. The organic species extracted from the catalysts were analyzed by GC-MS (Fig. 5).

The organic species initially produced on SAPO-35 (15 min) were mostly toluene, xylene and trimethylbenzene. As the reaction time increased to 32 min, the methanol conversion decreased from 98.49% to 76.37%, and organic species with a larger molecular size, such as naphthalene and methyl naphthalene, started to appear in the deposited coke species. When the reaction time was 83 min, the methanol conversion further decreased to 10.88%. Among the deposited coke species, the signals of naphthalene and methyl naphthalene obviously increased, and a small amount of multiple methylated naphthalene and anthracene dihydride appeared in addition to toluene, xylene and trimethylbenzene. The organic species during the early stage (21 min) of methanol conversion over SAPO-34 molecular sieve were mainly trimethylbenzene, tetramethylbenzene, naphthalene, methyl naphthalene and dimethyl naphthalene. When the reaction time was 72 min, the methanol conversion was still maintained at a high level (98.57%). Coke species such as tetramethylbenzene, naphthalene, methyl naphthalene and dimethylnaphthalene were enhanced, and new signals corresponding to trimethylnaphthalene, phenanthrene and pyrene appeared. At the stage of nearly complete deactivation of SAPO-34 (447 min, 33.46% methanol conversion), methyl benzene compounds disappeared. A significant change in the relative amounts of the other organic species occurred, and the polycyclic aromatic hydrocarbon

phenanthrene and pyrene and their methyl substituted derivatives became the major coke species. By comparing the evolution of the organic species in SAPO-35 and SAPO-34, a common characteristic is that the main organic species generated in the initial stage were methylated benzene compounds which gradually changed to bulky aromatic hydrocarbons. The final coke molecules in SAPO-34 were significantly larger than those in SAPO-35.

The hydrocarbon pool mechanism is a widely recognized MTO reaction mechanism. Much experimental results indicated that the multiply methylated benzene (methyl substituents > 3)

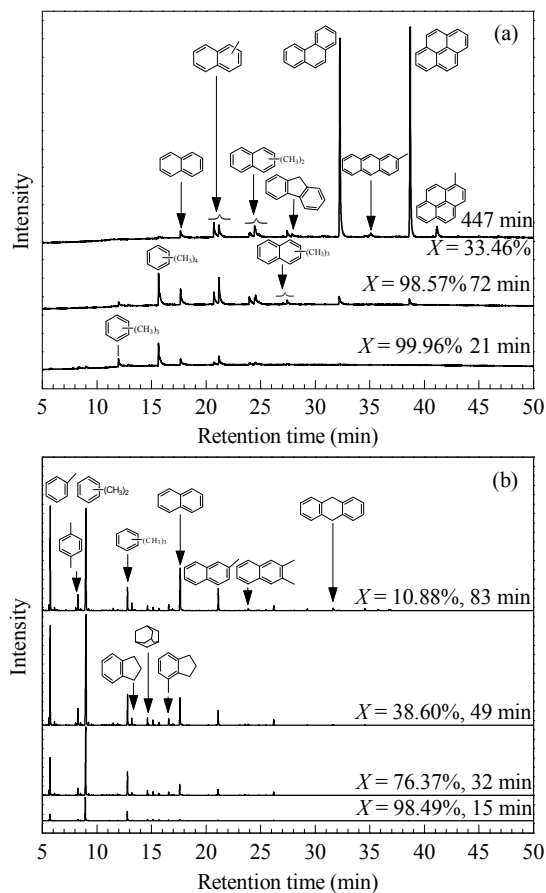


Fig. 5. Coke species in SAPO-34 (a) and SAPO-35 (b) in the MTO reaction. Reaction condition: WHSV = 4 h⁻¹, 400 °C, 40% CH₃OH solution; X refers to the CH₃OH conversion in the reaction.

Table 5

 Concentration of Brönsted acid sites in SAPO-35 molecular sieves calculated from ¹H MAS NMR.

Sample	B acid sites (mmol/g)
0.1Si	0.54
0.3Si	0.97
0.5Si	1.20

Graphical Abstract

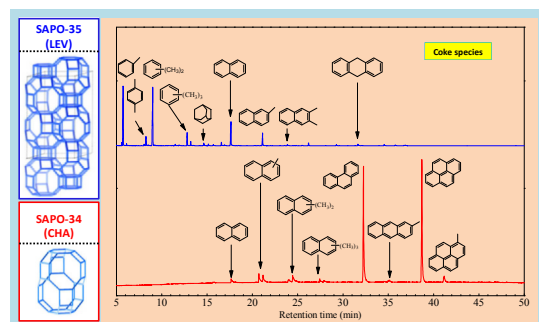
Chin. J. Catal., 2013, 34: 798–807 doi: 10.1016/S1872-2067(12)60557-9

Synthesis of SAPO-35 molecular sieve and its catalytic properties in the methanol-to-olefins reaction

LI Bing, TIAN Peng, LI Jinzhe, CHEN Jingrun, YUAN Yangyang, SU Xiong, FAN Dong, WEI Yingxu, QI Yue, LIU Zhongmin*

Dalian Institute of Chemical Physics, Chinese Academy of Sciences; University of Chinese Academy of Sciences

SAPO-35 was hydrothermally synthesized using hexamethylenimine as the template. The coke species in the MTO reaction over both SAPO-35 and SAPO-34 were investigated and correlated with their cage size.



is a hydrocarbon pool active center, on which the methylation of methanol/diethyl ether occurred to form ethylene and propylene, while the resulting less methylated benzene is re-methylated to start a new catalytic cycle [15,16,24–27]. In the present experiments, in the initial stage of reaction the existence of some hydrocarbon pool active species (multiply methylated benzenes) were observed in SAPO-34, whereas the coke species was dominated by less methylated benzenes in SAPO-35. With increased reaction time, at the stage of nearly complete deactivation, the main coke species in SAPO-34 were bulky aromatic hydrocarbons such as phenanthrene and pyrene (generated from ring condensation by hydrogen transfer from methylbenzene and methyl-naphthalene), while the coke species in SAPO-35 were methylbenzene, naphthalene and methyl-naphthalene. The difference in the coke species of SAPO-35 and SAPO-34 is probably related to their structures. The CHA cage of SAPO-34 (0.67 nm × 0.67 nm × 1.0 nm) is larger than the LEV cage of SAPO-35 (0.63 nm × 0.63 nm × 0.73 nm). The smaller cage of SAPO-35 restricted the formation of the hydrocarbon pool active species (multiply methylated benzene) and deactivated coke species (macromolecular fused-ring aromatic hydrocarbon). Also, it has a smaller accommodation capacity for deactivated coke species, which thus resulted in the rapid deactivation. The lack of hydrocarbon pool active species also led to the relatively low ethylene and propylene selectivity with SAPO-35. Moreover, it is worth noting that during the reaction, the organic compounds deposited in SAPO-35 always contained a small amount of saturated cyclo-alkane adamantane compounds. In our recent research on the coke species in SAPO-34 in the MTO reaction [28], we reported that adamantane compounds are the coke species in the low temperature reaction (≤ 350 °C), which were gradually transformed into naphthalene and substituted naphthalene species at elevated temperatures. In this experiment, the reaction temperature was 400 °C, so the existence of adamantane compounds in SAPO-35 once again demonstrated that the different cage size of the molecular sieve has a large influence on the generation and stability of the coke species.

4. Conclusions

SAPO-35 molecular sieves with different Si contents were

hydrothermally synthesized. The yield of solid sample increased with the increase of Si content in the synthesis gel. The crystallinity of the sample increased first and then decreased as the Si content increased. 0.3Si sample exhibited the highest crystallinity. The Si incorporation degree showed a dropping trend when the silica content rose. The surface of SAPO-35 crystals with a high silica content was rough. In particular, 1.0Si showed the characteristic of a core-shell structure, which could be due to secondary crystallization on the rough surface. SAPO-35 showed fast deactivation than SAPO-34 in the MTO reaction, and a higher silica content will cause faster deactivation. The main reason is that the higher Brönsted acid concentration in the sample with higher silica content led to more side reactions such as coke deposition and hydrogen transfer. By comparing and analyzing the deposited coke species formed in SAPO-35 and SAPO-34 during the MTO reaction, we concluded that the smaller cage of SAPO-35 limited the generation of hydrocarbon pool active species (polymethylbenzenes) and macromolecular coke species (polyaromatic hydrocarbons). Moreover, the smaller cage of SAPO-35 had a lower capacity to accommodate deposited coke species. These two reasons resulted in the faster deactivation of SAPO-35.

References

- [1] Lok B M, Messina C A, Patton R L, Gajek R T, Cannan T R, Flanigen E M. US Patent 4 440 871. 1984
- [2] Fu Y, Wang L F, Tan Y X, Ji H B. *Chem React Eng Technol*, 2000, 16(1): 55
- [3] <http://www.iza-structure.org/databases/>
- [4] Zhu Zh D, Hartmann M, Kevan L. *Chem Mater*, 2000, 12: 2781
- [5] Jeon H Y, Shin C H, Jung H J, Hong S B. *Appl Catal A*, 2006, 305: 70
- [6] Djieugoue M A, Prakash A M, Kevan L. *J Phys Chem B*, 2000, 104: 6452
- [7] Venkatathri N, Yoo J W. *Appl Catal A*, 2008, 340: 265
- [8] Cheung O, Liu Q L, Bacsik Z, Hedin N. *Microporous Mesoporous Mater*, 2012, 156: 90
- [9] Falconer J L, Li Sh G, Noble R D. US Patent 20050204916A1. 2005
- [10] Liu G Y, Tian P, Liu Zh M. *Progr Chem*, 2010, 22: 1531
- [11] Zhang J Ch, Zhang H B, Yang X Y, Huang Zh, Cao W L. *J Nat Gas Chem*, 2011, 20: 266
- [12] Liu G Y, Tian P, Xia Q H, Liu Zh M. *J Nat Gas Chem*, 2012, 21: 431
- [13] Nawaz S, Kolboe S, Stöcker M. *Stud Surf Sci Catal*, 1994, 81: 393

- [14] Chen J Sh, Wright P A, Thomas J M, Natarajan S, Marchese L, Bradley S M, Sankar G, Catlow C R A, Gai-Boyes P L. *J Phys Chem*, 1994, 98: 10216
- [15] Yuan C Y, Wei Y X, Li J Zh, Xu Sh T, Chen J R, Zhou Y, Wang Q Y, Xu L, Liu Zh M. *Chin J Catal*, 2012, 33: 367
- [16] Hereijgers B P C, Bleken F, Nilsen M H, Svelle S, Lillerud K P, Bjørgen M, Weckhuysen B M, Olsbye U. *J Catal*, 2009, 264: 77
- [17] Zhang F M, Kuang X H, Li L Sh, Shu X T, Wang W D, Qin F M, CN Patent 101 397 143. 2009
- [18] Guisnet M. *J Mol Catal A*, 2002, 182-183: 367
- [19] Guisnet M, Costa L, Ribeiro F R. *J Mol Catal A*, 2009, 305: 69
- [20] Prakash A M, Hartmann M, Kevan L. *Chem Mater*, 1998, 10: 932
- [21] Zhang D Zh. [PhD Dissertation]. Dalian: Dalian Institute of Chemical Physics, CAS, 2007
- [22] Sastre G, Lewis D W, Catlow C R A. *J Phys Chem*, 1996, 100: 6722
- [23] Liu G Y, Tian P, Zhang Y, Li J Zh, Xu L, Meng Sh H, Liu Zh M. *Microporous Mesoporous Mater*, 2008, 114: 416
- [24] Wang J D, Yu X B, Liu Y, Yang Y R. *Progr Chem*, 2009, 21: 1757
- [25] Arstad B, Kolboe S. *J Am Chem Soc*, 2001, 123: 8137
- [26] Arstad B, Kolboe S. *Catal Lett*, 2001, 71: 209
- [27] Lesthaeghe D, De Sterck B, Van Speybroeck V, Marin G B, Waroquier M. *Angew Chem, Int Ed*, 2007, 46: 1311
- [28] Wei Y X, Li J Zh, Yuan C Y, Xu Sh T, Zhou Y, Chen J R, Wang Q Y, Zhang Q, Liu Zh M. *Chem Commun*, 2012, 48: 3082